Journal of the Meteorological Society of Japan

EARLY ONLINE RELEASE

The DOI for this manuscript is
DOI:10.2151/jmsj.2021-054
J-STAGE Advance published date: May 14th, 2021

Evaluation of LMS6 and RS41 radiosonde humidity data obtained during YMC-Boreal Summer Monsoon study in 2018 and 2020

Kunio Yoneyama, Mikiko Fujita, Ayako Seiki, Ryuichi Shirooka, Satoru Yokoi,

Japan Agency for Marine-Earth Science and Technology (JAMSTEC), Yokosuka, Japan

Esperanza O. Cayanan,

Department of Science and Technology - Philippine Atmospheric Geophysical and Astronomical Services Administration (DOST-PAGASA), Quezon, Philippines

Cynthia O. Iglesia,

Laoag Synop Airport Upper Air Station, Department of Science and Technology - Philippine Atmospheric Geophysical and Astronomical Services Administration (DOST-PAGASA), Laoag, Philippines

and

Olivia C. Cabrera

Institute of Environmental Science and Meteorology, University of the Philippines, Diliman, Quezon, Philippines

December 2020 (submitted)
March 2021 (1st revision)
April 2021 (2nd revision)

---

1) Corresponding author: Kunio YONEYAMA, Japan Agency for Marine-Earth Science and Technology (JAMSTEC), 2-15, Natsushima-cho, Yokosuka, Kanagawa 237-0061 JAPAN.
Email: yoneyamak@jamstec.go.jp

Abstract

This short article describes humidity data correction based on intercomparison between the two manufacturers' radiosondes with the assessment using precipitable water vapor (PWV) derived from Global Navigation Satellite System (GNSS) signals. In addition, we propose a method to determine whether the same correction procedure can be applied for the case that such intercomparison cannot be conducted.

During the intensive observation called Years of the Maritime Continent - Boreal Summer Monsoon study in 2018 (YMC-BSM 2018), intercomparison of radiosonde between Lockheed Martin LMS6 and Vaisala RS41-SGP was conducted at Laoag, Ilocos Norte, Philippines from late July to early August 2018. While their mean difference of relative humidity (RH) showed better than 5%, dry bias was confirmed for LMS6 only during clear sky daytime soundings based on the comparison of PWV with that derived from GNSS signals. To use different radiosonde data with the same research-quality, we developed a correction table for LMS6 RH data.

While a direct intercomparison between different radiosondes and independently developed observational tools such as GNSS-receiver is ideal to evaluate the data quality, it is not always able to be performed. Indeed, we obtained LMS6 radiosonde data at different site at Yap Island, Federated States of Micronesia from another field campaign

YMC-BSM 2020, where any intercomparison could not be conducted. In order to decide whether the same correction procedure obtained from YMC-BSM 2018 can be applied to those data, we assessed their similarity based on a relationship between specific humidity from surface meteorological station data that was obtained independently prior to launch and radiosonde specific humidity averaged over 300 m from the initial radiosonde measurement point. This method allowed us to confirm the same behavior between Laoag data in 2018 and Yap data in 2020, thus we applied our correction method to RH data in YMC-BSM 2020.

Keywords: YMC; field campaign; radiosonde humidity bias

1. Introduction

Radiosonde is a basic observation tool to measure atmospheric vertical profiles and is often used in the field campaigns, since it can capture the characteristics of the atmospheric structure at high vertical resolution (raw data are taken every 4 - 6 m interval). Besides, it is well-known that additional radiosonde soundings greatly improve analysis fields (Moteki et al. 2011) and forecast skill (Inoue et al. 2015) through the use of data assimilation. The international field program, Years of the Maritime Continent or YMC has been carried out since 2017 (Yoneyama and Zhang 2020). YMC is a unique attempt to understand weather and climate systems over the Maritime Continent through two different field observational approaches; intensive observation focusing on specific phenomena with limited observation period and long-term measurement done by the local meteorological agencies or special observation tool deployment including mooring system, unmanned autonomous vehicles and so on. For the most cases, radiosonde is used. The accurate moisture distribution and variation obtained by radiosonde are crucial to understand dominant atmospheric convective variabilities such as diurnal cycle of rain, the Madden-Julian Oscillation, and the boreal summer intraseasonal oscillation over the Maritime Continent and adjacent seas, where the atmospheric convection is the most active over the world (Neelin and Held 1987; Sobel et al. 2001; Yamanaka 2016; Yoneyama and Zhang 2020). While the radiosonde data are believed to be accurate as an in-situ measurement system, it is often reported that their

83 relative humidity data contain erroneous data mainly caused by solar heating of humidity
84 sensor from the research-quality viewpoint (e.g., Vömel et al. 2007a; Yoneyama et al. 2008).
85 In addition, their accuracy varies with radiosonde manufacturers (Ciesielski et al. 2010; Nash
86 et al. 2011). Figure 1 shows a map of radiosonde type used during the two field campaigns
87 in 2018 and 2020 as shown later. During the campaign, the Vaisala RS41 and Lockheed
88 Martin LMS6 radiosondes were employed. When we analyze those data, it is important that
89 any scientific knowledge obtained using those data should be the same regardless of
90 radiosonde type (LMS6 or RS41). Thus, we need to reduce possible errors as much as
91 possible. Ciesielski et al. (2012) provided a guideline of general procedure for producing
92 research-quality radiosonde sounding data from field campaigns. They proposed to adopt a
93 naming convention for those procedures from level-1 to level-4 in addition to original (raw)
94 datasets as level-0. The level-1 indicates data in a common format regardless of their
95 original data types and systems. Then, data processed with automated quality-control
96 algorithms, which remove apparent errors, are labeled as level-2. The level-3 procedure is
97 required to identify and reduce systematic errors or biases in the high (original) vertical
98 resolution data. Level-4 datasets can be obtained from level-3 datasets by producing data
99 at uniform vertical resolution (e.g., 5 hPa) with quality-control information flags. In these
100 procedures, they emphasized the importance and difficulty of humidity data bias
101 identification and reduction. Since the radiosonde data taken as part of the YMC are used

by many researchers who did not conduct observations by themselves, data quality should be evaluated by the researchers who conducted the field experiment. Thus, this is a report about the quality control of data from those who conducted field campaigns in 2018 and 2020.

In this study, we will first show the result of data quality evaluation based on the intercomparison done during the field campaign at Laoag, Ilocos Norte, Philippines in July - August 2018 in Section 2. Then, we will apply the same correction procedure developed from the 2018 campaign onto another field campaign data taken in 2020 at different site, Yap, Federated States of Micronesia based on the identification of possible bias (Section 3). This procedure contains a suggestion of humidity data correction for the case that direct intercomparison cannot be performed during the campaign. A brief summary and remarks for data quality procedure are provided in Section 4.

2. Intercomparison during the YMC-BSM 2018

A field experiment to study boreal summer monsoon was conducted as YMC-Boreal Summer Monsoon study in 2018 (YMC-BSM 2018) at various sites in the tropical western Pacific region, where unique local phenomena are often observed. The details of the campaign are found in their website (http://www.jamstec.go.jp/ymc/campaigns/IOP_YMC-BSM_2018.html). One key research topic is to study a mechanism of offshore propagation

121 of diurnally-developed atmospheric convections along the coast and its relation to large-
122 scale atmospheric disturbances known as the northward propagating Boreal Summer
123 Intraseasonal Oscillation (BSISO). For this purpose, four radiosoundings were performed
124 per day at Laoag (18.18N, 120.53E), Province of Ilocos Norte, Philippines during July 1 -
125 August 31, 2018. While the Lockheed Martin LMS6 or Graw DFM-09 radiosonde is usually
126 used at the Laoag synop airport upper air station, only LMS6 was used during two months
127 of YMC-BSM 2018 period to avoid inconsistency of radiosonde data. In addition,
128 intercomparison among different types of radiosonde was conducted to evaluate their
129 relative differences, so that such information can be used when we use the same type of
130 radiosonde data taken at different sites. As shown in the next section and in Fig. 1, we also
131 utilized LMS6 radiosonde data taken at Yap (9.50N, 138.08E) and Palau (7.37N, 134.54E),
132 as well as Vaisala RS41-SGP (RS41) onboard the research vessel (R/V) Mirai (12.00N,
133 135.00E) and Legazpi (13.15N, 123.73E), Province of Albay, Philippines, during the YMC-
134 BSM 2020 campaign. In this study, we will focus on the evaluation of LMS6 radiosonde
135 humidity data, which are used for both the campaigns. Since the processing software of
136 LMS6 is different for the various sites and it may also affect the results, their software version
137 information is provided in Table 1. As shown, while LMS6 transmitter is used at Yap, they
138 use the U.S. National Oceanic and Atmospheric Administration (NOAA)'s original software
139 "Radiosonde Replacement System (RRS) Workstation Software (RWS)" (NOAA, 2018). In

addition, we used relatively new sensors (within a year from their production) to avoid possible errors from sensor aging.

To evaluate LMS6 radiosonde humidity data, intercomparison between LMS6 and RS41 was performed by launching both radiosondes simultaneously for 20 times during July 27 - August 3, 2018 (Table 2). It should be noted that while we attached them 1m apart using a plastic rod and launched using a single balloon at 0300 and 0900 UTC, we launched them simultaneously but separately using two balloons at 0000 and 0600 UTC. This is because we kept the same launching procedure for 6-hourly sounding using LMS6 during the entire 2-month YMC-BSM 2018 campaign period. Unfortunately, two soundings had failed to obtain data correctly for intercomparison, thus 18 sounding data (13 in daytime, 5 in evening) were used. In addition, during this period a Global Navigation Satellite System (GNSS) receiver was installed at the Laoag weather station to measure precipitable water vapor (PWV; Rocken et al. 1993). The procedure to derive PWV from GNSS signal is the same as that shown in Fujita et al. (2008, 2020), who reported the mean difference with radiosonde-derived PWV is better than 1mm with a root mean square error of 2-3 mm.

The result of intercomparison between LMS6 and RS41 is shown in Fig. 2. It should be noted that the intercomparison was performed under clear sky condition as shown in Table 2. Note that here we use the term “clear sky” not as cloud amount “0” but as within fewer clouds condition ranging 1-3 except one case of 4 at sounding number 15 in Table 2. Relative

159 humidity (RH) profiles of LMS6 show dry bias comparing to that of RS41 for entire
160 troposphere (mean difference between the two radiosondes in the 1000-200 hPa layer is
161 3.9%, and the difference increases with height in the upper troposphere above 200 hPa
162 level) during daytime sounding (Fig. 2a), while such difference cannot be found in the
163 evening soundings (Fig. 2b). Actually, we cannot conclude that LMS6 has dry bias only from
164 this figure, as RS41 may have a wet bias. Note that if we assume that RS41 data is correct
165 (no wet nor dry bias), the difference of 3.9% is ranged within the LMS6 specified accuracy
166 (+/-5%), suggesting that such a difference is acceptable from the operational-use viewpoint.
167 Having said that, the same quality among different types of radiosonde is desirable
168 especially when the researchers use them to calculate a moisture flux in a certain domain
169 or discuss humidity variation using the different radiosonde data. As one index which can be
170 obtained independently from the radiosonde measurement, a comparison of PWV derived
171 from two sources; radiosonde and GNSS, is useful. Indeed, previous studies demonstrated
172 the usefulness of GNSS-derived PWV for assessing radiosonde humidity data validation
173 (Wang and Zhang 2008; Wang et al. 2013). Figure 3 shows PWV differences between
174 GNSS-PWV and Radiosonde-PWV for LMS6 (Fig. 3a) and RS41 (Fig. 3b), respectively. We
175 can confirm that the difference between GNSS and RS41-derived PWV is smaller than 1
176 mm (e.g., mean difference at 14 LST is -0.92 mm with a standard deviation of 1.1 mm)
177 regardless of the time of the day, while LMS6 shows large dry bias in daytime (the difference

178 at 14 LST is -3.8 mm with a standard deviation of 1.2 mm). The difference found in RS41
179 and GNSS is comparable to the previous works (e.g., Realini et al. 2014), which compared
180 GNSS-PWV with Vaisala RS92-derived PWV, but the data consistency between RS92 and
181 RS41 are confirmed by several works (e.g., Jensen et al. 2016; Kawai et al. 2017). Based
182 on this result, we decided that RS41 humidity data is more reliable than that obtained by
183 LMS6, and we will use RS41 as a reference for RH data correction of LMS6.

184 Here, before describing correction procedure, we discuss possible causes of the biases
185 briefly. The clear contrast between the daytime and evening suggests that the differences
186 between the two radiosonde types in the daytime soundings are caused by daytime solar
187 radiation (Vömel et al. 2007a), although LMS6 has a sunshade to protect from solar radiation
188 as much as possible. Since the difference can be found from the ground surface, it is
189 possible to speculate that exposure under the sunshine prior to launch about 5 minutes or
190 more might result in some portions of this dryness. Besides, it is also possible to speculate
191 that sunshade could not fully prevent from solar radiation during ascent with slight inclination
192 rather than upright. Larger differences above 200 hPa might reflect the fact that all
193 radiosondes launched during the intercomparison period encountered strong winds over 10
194 m s^{-1}(not shown), which might result in such sunshade could not prevent from the solar
195 radiation due to inclination. There are also several other possible reasons to explain the
196 difference. For example, we cannot exclude a possible error source by the slow sensor

197 response at low temperatures, known as a time-lag error (Miloshevich et al. 2004). However,
198 it is impossible to quantify the biases due to the time-lag error, as we do not have information
199 about the sensor time constant which is determined by the manufacturer on the basis of
200 dedicated measurements in a laboratory environment. Instead, what we can do is to
201 minimize their gap between RS41 and LMS6 in producing seamless humidity datasets
202 based on the fact that the differences exist only in clear sky daytime soundings.

203 As for correction schemes, several methods have been proposed and used for previous
204 field campaigns (e.g., Nuret et al. 2008; Ciesielski et al. 2014). If we could obtain the
205 simultaneous sounding data using chilled-mirror type hygrometers such as Snow-white
206 (Fujiwara et al. 2003) or cryogenic frost-point hygrometer (Vömel et al. 2007b) with enough
207 sample numbers, a polynomial fitting with those data profiles might be better. However, we
208 did not launch such hygrometers during the 2018 campaign. Thus, by assuming that RH of
209 RS41 is better than that of LMS6 during the 2018 campaign as mentioned above, we fitted
210 LMS6 RH data to that of RS41 using the cumulative distribution function (CDF) matching
211 method, which produces a look-up table for humidity bias correction (Nuret et al. 2008;
212 Ciesielski et al. 2009). Since we could not find significant difference between 1100 LT and
213 1400 LT sounding cases, we simply calculated CDF matching using all 13 samples for
214 daytime sounding. RH bias as a function of RH and temperature is shown in Fig. 4. Then,
215 bias correction is performed onto the RHs and its result is shown in Fig. 5, which

demonstrates that the humidity correction performed well for entire troposphere. Figure 6, which shows the frequency distribution of occurrence of RH for original/corrected values, provides the same information with Fig. 5, but it also tells how this correction works. The peak of frequency in the higher RH range, which is located at 65-75% in the original LMS6 data, shifts to 75-85% in the corrected one, while another peak around 20-30% in the original LMS6 disappears in the corrected distribution. The former may capture moist condition in the lower troposphere over the warm pool, while the latter corrected dry bias in the upper troposphere mainly above 200 hPa shown in Fig. 2a.

3. Application of correction scheme to another field campaign data

Although we obtained the quality-controlled LMS6 humidity data during the YMC-BSM 2018 campaign period, it does not guarantee such correction is valid for other LMS6 data, as the system has been improved by the manufacturer's effort and minor changes of the system is often done without notice to the users.

In the boreal summer in 2020 (August - early September), another YMC field campaign called YMC-Boreal Summer Monsoon study in 2020 (BSM 2020) was conducted. During this campaign period, a radiosonde network was formed by three land-based sites and the R/V Mirai (indicated in blue in Fig. 1). While RS41 was used at Legazpi and onboard the R/V Mirai, LMS6 was used at two sites; Yap, Federated States of Micronesia, and Palau. At

these land-based sites, the twice daily operational radiosoundings were increased four times per day a six-hour interval during the campaign period. As for LMS6 data at these sites, is it possible to use their data without any correction? Or, is it acceptable to adopt the same correction procedure obtained from the YMC-BSM 2018 Laoag site as shown in the previous section? All what we obtained from those sites are only original high-resolution (every 1 second) radiosonde data, and we did not conduct any intercomparison there.

One idea to answer to above is the use of surface meteorology data taken independently using their surface weather station as initial ground surface data prior to launch. It is expected that specific humidity at the surface measured by the weather station and in a well-mixed boundary layer measured by the radiosonde should be close each other. For example, Fitzjarrald and Garstang (1981) suggested the difference are between 1.0 - 1.5 g/kg from tropical Atlantic Ocean experiment. However, since the LMS6 data obtained at Laoag during the YMC-BSM 2018 showed dry bias even in the boundary layer (Fig.2a), it is expected that their difference may be larger. Figure 7 shows scatter plot of the specific humidity measured at the surface (Q_SFC) and that averaged over 300m from the radiosonde initial data point (Q_BL). Mean difference between Q_SFC and original Q_BL for daytime sounding (2.31 g/kg) is higher than that for evening sounding (0.88 g/kg), and the contrast (1.43 g/kg) is comparable to the LMS6's dry bias of about 5% with respect to RS41 in the lower troposphere. The RH correction for daytime soundings improves the mean difference

254 between Q_SFC and Q_BL to 1.14 g/kg that is close to that for evening soundings.

255 Then, we also calculated the same scatter plot for all data obtained during YMC-BSM
256 2018 period (Fig. 8). Here, it should be noted that although similar comparison between
257 surface and boundary layer was used to detect dry bias and correction was applied to all
258 data for the TOGA-COARE (Tropical Ocean Global Atmosphere - Coupled Ocean-
259 Atmosphere Response Experiment) field experiment (Zipser and Johnson 1998; Lucas and
260 Zipser 2000), it is different from our case. For TOGA-COARE data, solar radiation-induced
261 error is one of error sources, but the chemical contamination between the humidity sensor
262 and the radiosonde package material mainly caused dry bias for Vaisala RS80 radiosonde
263 data (Wang et al. 2002). Namely, such dry bias appeared in all sounding data. On the other
264 hand, the dry bias studied here is mainly caused by daytime solar radiation. Thus, a
265 correction scheme developed here can be applied only to data taken during daytime. In
266 addition, when the daytime data are obtained under heavy clouds or rainy days, it may not
267 be necessary to be corrected. As noted in Table 2, the intercomparison was conducted only
268 under clear sky condition. In other words, we should not apply the correction scheme
269 obtained from the intercomparison at YMC-BSM 2018 to the data obtained in cloudy/rainy
270 days. In this study, we identified cloudy/rainy days using a threshold of 93% RH following to
271 Zuidema (1998). When the data show RH higher than 93% and have enough thickness
272 (thicker than 30 hPa) between 800 hPa and 300 hPa, we identified the sounding site is

273 covered with cloud, whose threshold thickness (30 hPa) was determined based on several
274 trials to detect the most similar value with that of non-daytime period. Note that, however,
275 their difference is not changed much from those layer-thickness selections, because it is
276 often covered with thick layers due to rain when several points show the values higher than
277 93% RH (not shown). We confirmed that all daytime soundings shown in Table 2 were not
278 categorized in this cloudy/rainy condition defined using RH threshold. Also, note that the
279 range starting from 800 hPa was chosen to surely avoid the top of boundary mixed layer,
280 where high RH often appears, and cloudy layer from spotted/scattered shallow clouds. Thus,
281 in Fig. 8, we plotted specific humidity at the surface and 300 m-layer mean before/after
282 correction for three different cases: clear sky daytime, cloudy/rainy daytime, and others
283 (evening - night). Those are indicated in different colors and shapes. Namely, only data taken
284 during clear sky daytime were corrected (indicated in red and magenta). Indeed, we
285 confirmed that the mean difference between Q_SFC and Q_BL during cloudy/rainy daytime
286 (1.30 g/kg) is significantly lower than that of clear sky daytime (2.20 g/kg), and rather very
287 close to that of the others (1.23 g/kg).

288 Then, the similar plot was calculated for the data obtained at Yap during August 6 -
289 September 9, 2020 (Fig. 9). We can confirm the similar difference and relationship for Yap
290 LMS6 data. The mean difference between Q_SFC and Q_BL for clear sky daytime
291 soundings (2.49 g/kg), which is close to that for Laoag BSM2018 case (2.20 g/kg), is

292 significantly higher than that for cloudy/rainy daytime soundings (1.32 g/kg), which is also
293 close to that for the Laoag case (1.30 g/kg). Namely, it is possible to recognize that LMS6
294 used at Yap may have similar dry bias with that in YMC-BSM 2018 and the same correction
295 procedure can be applied, despite the data processing software is different (Table 1).
296 According to the data policy of the YMC, we are required to provide quality-controlled data
297 to the public within one year from the completion of the field campaign. Thus, when we
298 release those YMC-BSM 2020 radiosonde data, they will be labeled as levels-3 and 4
299 (Ciesielski et al. 2012) with notation of such humidity correction based on YMC-BSM 2018
300 intercomparison result.
301
302 **4. Summary and concluding remarks**
303 This article reported the evaluation of LMS6 radiosonde humidity data obtained during the
304 YMC-BSM 2018 campaign at Laoag, Ilocos Norte, Philippines based on the intercomparison
305 with simultaneous observation with RS41 radiosonde and comparison of PWV derived from
306 radiosonde and GNSS signal. LMS6 showed a dry bias of approximately 4%RH or so
307 comparing to RS41 in the entire troposphere with higher difference above 200 hPa level.
308 Such differences were confirmed only during the clear sky daytime soundings and
309 recognized that they were caused by humidity sensor heating due to solar radiation. Since
310 the comparison of PWV derived from radiosondes and GNSS showed that RS41-derived

311 PWV was closer to GNSS-derived one, we decided to correct LMS6 bias using RS41 data.
312 The CDF matching method was applied to deduce correction values of LMS6 RH data
313 against RS41 as a function of observed RH and temperature.

314 In addition to the YMC-BSM 2018 data, we obtained LMS6 data from another field
315 campaign YMC-BSM 2020. In this study, we showed the case of data taken at Yap,
316 Federated States of Micronesia during August - September 2020. Note that although we
317 obtained LMS6 data from Palau, currently we have not obtained their surface meteorological
318 data taken independently. Thus, we focused only Yap data in this study. However, as noted
319 in Table 1, since Palau adopts the similar system with Laoag, we expect the current study
320 can be applied to them.

321 Since we do not have any intercomparison between LMS6 and RS41 data during the
322 YMC-BSM 2020 campaign period, we proposed to use a relationship between the surface
323 specific humidity data and mean specific humidity data averaged over 300m in the boundary
324 layer as one possible index to judge whether the correction scheme developed for YMC-
325 BSM 2018 can be used for the 2020 case or not, since the surface value is obtained
326 independently from the radiosonde at most stations. Based on the qualitative similarity (their
327 mean difference is the same order for both campaigns, and at least we confirmed that the
328 mean difference between Q_SFC and Q_BL for clear sky daytime soundings was
329 significantly higher than that for cloudy/rainy daytime soundings as Laoag case showed),

330 we decided to apply the same correction scheme onto the Yap LMS6 sounding data. This
331 suggests that it is possible to apply the same procedure to other sites, where
332 intercomparison or any other evaluation mechanism have not been established, once the
333 correction values for the same type of radiosonde have been determined at other sites.
334 Besides, we used RH values to detect cloudy/rainy conditions during the sounding (judged
335 as cloudy/rainy, if 93% or higher RH appears over 30 hPa thickness between 800 hPa and
336 300 hPa), so that the humidity correction associated with solar radiation in daytime can be
337 applied only to affected data under clear sky days.

338 The datasets used in this study are available from the YMC data archive site at
339 http://www.jamstec.go.jp/ymc/ymc_data.html, and a look-up table for LMS6 is also available
340 in the same site and Supplement. It should be noted again that this look-up table for LMS6
341 can be used only for the data taken during clear sky daytime.

342 Currently, the authors have also been conducting to develop correction scheme for other
343 radiosonde types such as Graw obtained at Laoag. We believe those efforts should be done
344 in collaboration with the local meteorological agencies, so that not only the field campaign
345 data but also operational routine data can be used for weather and climate studies with high
346 research-quality.

347

348

Acknowledgments

The authors would like to express our sincere thanks to all the staff of Laoag synop airport upper air station for their radiosonde sounding operation for the YMC-BSM 2018 campaign as well as Dr. Vicente B. Malano, Dr. Landrico U. Dalida, Jr., and Dr. Flaviana D. Hilario at the Headquarters of PAGSA for their support and allowance of this collaborative observation. Many students from the University of the Philippines - Diliman also helped the work at Laoag. We also thank Mr. Souichiro Sueyoshi, a technical staff from Nippon Marine Enterprise Co. Ltd., for his support to the intercomparison experiment at Laoag. We also appreciate the U.S. National Oceanic and Atmospheric Administration, Yap Weather Services, and Palau Weather Services for their enhanced radiosonde observations during the YMC-BSM 2020. The constructive comments from two anonymous reviewers and Prof. M. D. Yamanaka that helped to improve the manuscript are greatly appreciated.

References

Ciesielski, P. E., R. H. Johnson, and J. Wang, 2009: Correction of humidity biases in Vaisala RS80-H sondes during NAME. *J. Atmos. Oceanic Technol.*, **26**, 1763-1780.

Ciesielski, P. E., W.-M. Chang, S.-C. Huang, R. H. Johnson, B. J.-D. Jou, W.-C. Lee, P.-H. Lin, C.-H. Liu, and J. Wang, 2010: Quality-controlled upper-air sounding dataset for TiMREX/SoWMEX: Development and corrections. *J. Atmos. Oceanic Technol.*, **27**, 1802-1821.

Ciesielski, P. E., P. T. Haertel, R. H. Johnson, J. Wang, and S. M. Loehrer, 2012: Developing high-quality field program sounding datasets. *Bull. Amer. Meteor. Soc.*, 93, 325–336.

Ciesielski, P. E., H. Yu, R. H. Johnson, K. Yoneyama, M. Katsumata, C. N. Long, J. Wang, S. M. Loehrer, K. Young, S. F. Williams, W. Brown, J. Braun, and T. Van Hove, 2014: Quality-controlled upper-air sounding dataset for DYNAMO/CINDY/AMIE: Development and corrections. *J. Atmos. Oceanic Technol.*, **31**, 741-764.

Fitzjarrald, D. R., and M. Garstang, 1981: Vertical structure of the tropical boundary layer. *Mon. Wea. Rev.,* **109,** 1512–1526.

Fujita, M., F. Kimura, K. Yoneyama, and M. Yoshizaki, 2008: Verification of precipitable water vapor estimated from shipborne GPS measurements. *Geophys. Res. Lett.*, **35**, L13803, doi:10.1029/2008GL033764.

Fujita, M., T. Fukuda, I. Ueki, Q. Moteki, T. Ushiyama, and K. Yoneyama, 2020: Experimental

382 observations of precipitable water vapor over the open ocean collected by autonomous
383 surface vehicles for real-time monitoring applications. *SOLA*, **16A**. 19-24.
384 Inoue, J., A. Yamazaki, J. Ono, K. Dethloff, M. Maturilli, R. Neuber, P. Edwards, and H.
385 Yamaguchi, 2015: Additional Arctic observations improve weather and sea-ice forecasts
386 for the Northern Sea Route. *Sci. Rep.*, **5**, 16868. doi:10.1038/srep16868.
387 Jensen, M. P., D. J. Holdridge, P. Survo, R. Lehtinen, S. Baxter, T. Toto, and K. L. Johnson,
388 2016: Comparison of Vaisala radiosondes RS41 and RS92 at the ARM Southern Great
389 Plains site. *Atmos. Meas. Tech.*, **9**, 3115-3129.
390 Kawai, Y. M. Katsumata, K. Oshima, M. E. Hori, and J. Inoue, 2017: Comparison of Vaisala
391 radiosondes RS41 and RS92 launched over the oceans from the Arctic to the tropics.
392 *Atmos. Meas. Tech.*, **10**, 2485-2498.
393 Lucas ,C., and E. J. Zipser, 2000: Environmental variability during TOGA COARE. *J. Atmos.*
394 *Sci*., **57**, 2333-2350.
395 Miloshevich, L. M., A. Paukkunen, H. Vömel, and S. J. Oltmans 2004: Development and
396 validation of a time-lag correction for Vaisala radiosonde humidity measurements. *J.*
397 *Atmos. Oceanic Technol*., **21**, 1305-1327.
398 Moteki, Q., K. Yoneyama, R. Shirooka, H. Kubota, K. Yasunaga, J. Suzuki, A. Seiki, N. Sato,
399 T. Enomoto, T. Miyoshi, and S. Yamane, 2011: The influence of observations propagated
400 by convectively coupled equatorial waves. *Quart. J. Roy. Meteor. Soc.*, **137**, 641-655.

401 Nash, J., T. Oakley, H. Vomel, and W. Li, 2011: WMO intercomparison of high quality
402 radiosonde systems. WMO/TD-No. 1580, Instruments and Observing Methods, Rep. 107,
403 238 pp.
404 National Oceanic and Atmospheric Administration (NOAA), 2018: Radiosonde Replacement
405 System (RRS) Workstation user guide for RWS software version 3.4.0.2. U.S.
406 Department of Commerce, NOAA, National Weather Services Headquarters, Field
407 Systems Operations Center, Observing Systems Branch. (Ed.), pp.334. Available from
408 https://www.weather.gov/upperair/RRS.
409 Neelin, J. D., and I. M. Held, 1987: Modeling tropical convergence based on the moist static
410 energy budget. *Mon. Wea. Rev*., **115**, 3-12.
411 Nuret, M., J.-P. Lafore, O. Bock, F. Guichard, A. Agusti-Panareda, J.-B. N'Gamini, and J.-L.
412 Redelsperger, 2008: Correction of humidity bias for Vaisala RS80-A sondes during the
413 AMMA 2006 observing period. *J. Atmos. Oceanic Technol.,* **25,** 2152–2158.
414 Realini, E., K. Sato, T. Tsuda, Susilo, and T. Manik, 2014: An observation campaign of
415 precipitable water vapor with multiple GPS receivers in western Java, Indonesia. *Prog.*
416 *Earth Planet. Sci.*, **1**, 17.
417 Rocken, C., R. Ware, T. Van Hove, F. Solheim, C. Alber, J. Johnson, M. Bevis, and S.
418 Businger, 1993: Sensing atmospheric water vapor with the global positioning system.
419 *Geophys. Res. Lett.*, **20**, 2631–2634.

420 Sobel, A. H., J. Nilsson, and L. M. Polvani, 2001: The weak temperature gradient
421 approximation and balanced tropical moisture waves. *J. Atmos. Sci.*, **58**, 3650–3665.
422 Vömel, H., H. Selkirk, L. Miloshevich, J. Valverde-Canossa, J. Valdés, E. Kyrö, R. Kivi, W.
423 Stolz, G. Peng, and J. A. Diaz, 2007a: Radiation dry bias of the Vaisala RS92 humidity
424 sensor. *J. Atmos. Oceanic Technol*., **24**, 953-963.
425 Vömel, H., D. David, and K. Smith, 2007b: Accuracy of tropospheric and stratospheric water
426 vapor measurements by the cryogenic frost point hygrometer: Instrumental details and
427 observations. *J. Geophys. Res*., **112**, D08305, doi:10.1029/2006JD007224.
428 Wang, J., H. L. Cole, D. J. Carlson, E. R. Miller, K. Beierle, A. Paukkunen, and T. K. Laine,
429 2002: Corrections of humidity measurement errors from the Vaisala RS80 Radiosonde-
430 application to TOGA COARE data. *J. Atmos. Oceanic Technol*., **19**, 981-1002.
431 Wang, J., and L. Zhang, 2008: Systematic errors in global radiosonde precipitable water
432 data from comparisons with ground-based GPS measurements. *J. Climate*, **21**, 2218-
433 2238.
434 Wang, J., L. Zhang, A. Dai, F. Immler, M. Sommer, and H. Vömel, 2013: Radiation dry bias
435 correction of Vaisala RS92 humidity data and its impacts on historical radiosonde data. *J.*
436 *Atmos. Oceanic Technol*., **30**, 197-214.
437 Yamanaka, M. D., 2016: Physical climatology of Indonesian maritime continent: An outline
438 to comprehend observational studies. *Atmos. Res.*, **178-179**, 231-259.

Yoneyama, K., M. Fujita, N. Sato, M. Fujiwara, Y. Inai, and F. Hasebe, 2008: Correction for radiation dry bias found in RS92 radiosonde data during the MISMO field experiment. *SOLA*, **4**, 13-16.

Yoneyama, K. and C. Zhang, 2020: Years of the Maritime Continent. *Geophys. Res. Lett.*, **47**, e2020GL087182.

Zipser, E. J., and R. H. Johnson, 1998: Systematic errors in radiosonde humidities: A global problem? Preprints, *10th Symposium on Meteorological Observations and Instruments*, 11-16 Jan. 1998, Phoenix, AZ, USA. Amer. Meteor. Soc., 72-73.

Zuidema, P., 1998: The 600-800-mb minimum in tropical cloudiness observed during TOGA COARE. *J. Atmos. Sci*., **55**, 2220-2228.

451 List of Table and Figures

Fig. 4. RH difference between LMS6 and RS41 as a function of RH and temperature based on CDF matching method. Dotted line indicates the saturation with respect to ice.

Fig. 5. Same as Fig. 2a, but for corrected values based on CDF matching method.

Fig. 6. Frequency distribution of RH binned by 5% for original LMS6 (black), corrected LMS6 (red), and original RS41 (blue). This plot was made using 5hPa interval data between 1000 hPa and 80 hPa from the 13 daytime soundings.

Fig. 7. Scatter plots of specific humidity as a function of surface value measured by surface meteorological station and 300m-mean value above radiosonde initial point for (a) before, and (b) after RH correction. Numbers indicate mean difference (Diff) and square root of unbiased variance from the mean difference (sq(u2)) for 13 daytime soundings and 5 evening soundings in g/kg unit. Since correction is not applied onto non-daytime sounding, “others” in both figures are the same.

Fig. 8. Same as Fig. 7, but for entire 2 months period during the YMC-BSM 2018. Red/magenta colors indicate the data taken during clear sky daytime for before/after RH correction. Green indicates data taken during cloudy/rainy daytime, while blue indicates evening and nighttime. Clear sky and cloudy/rainy daytime are defined using 93% RH threshold. See more details in the text.

Fig. 9. Same as Fig.8, but for the data obtained at Yap during the YMC-BSM 2020.

Table 1. Software version for data processing in the ground system used in this study.

Site	Transmitter Type	Ground System Software Version
Laoag	Vaisala RS41-SGP Lockheed Martin LMS6	MW41 2.3.0 LMG6 Win9000 6.3.1
Yap	Lockheed Martin LMS6	NOAA RWS 3.4.0.2
Palau	Lockheed Martin LMS6	LMG6 Win9000 6.6.0

Table 2. Date and time of intercomparison between LMS6 and RS41 at Laoag (18.18N, 120.53E). Cloud amount is taken from surface synoptic observation (SYNOP) report at PAGASA Laoag station, and they are expressed in okta (eighths of the sky).

No.	Nominal Time (UTC)	Actual launch time (LT)	Remarks
1	2018.07.27 09:00	2018.07.27 16:36	Cloud amount (3)
2	2018.07.28 03:00	2018.07.28 10:33	Cloud amount (1)
3	2018.07.28 09:00	2018.07.28 16:32	Cloud amount (3)
4	2018.07.29 03:00	2018.07.29 10:35	Cloud amount (3)
5	2018.07.29 06:00	2018.07.29 13:34	Cloud amount (3)
6	2018.07.29 09:00	2018.07.29 16:35	Cloud amount (1)
7	2018.07.30 03:00	2018.07.30 10:44	Cloud amount (2)
8	2018.07.30 06:00	2018.07.30 13:31	Cloud amount (1)
9	2018.07.30 09:00	2018.07.30 16:35	Cloud amount (1)
10	2018.07.31 03:00	2018.07.31 10:35	Cloud amount (2)
11	2018.07.31 06:00	2018.07.31 13:33	Cloud amount (1)
12	2018.07.31 09:00	2018.07.31 16:31	Cloud amount (2)
13	2018.07.31 12:00	2018.07.31 19:31	Cloud amount (2) Data are unavailable
14	2018.08.01 03:00	2018.08.01 10:40	Cloud amount (3)
15	2018.08.01 06:00	2018.08.01 13:30	Cloud amount (4)
16	2018.08.02 00:00	2018.08.02 07:38	Cloud amount (1) Data are unavailable
17	2018.08.02 03:00	2018.08.02 10:32	Cloud amount (2)
18	2018.08.02 06:00	2018.08.03 13:30	Cloud amount (1)
19	2018.08.03 03:00	2018.08.03 10:31	Cloud amount (1)
20	2018.08.03 06:00	2018.08.03 13:30	Cloud amount (3)

500

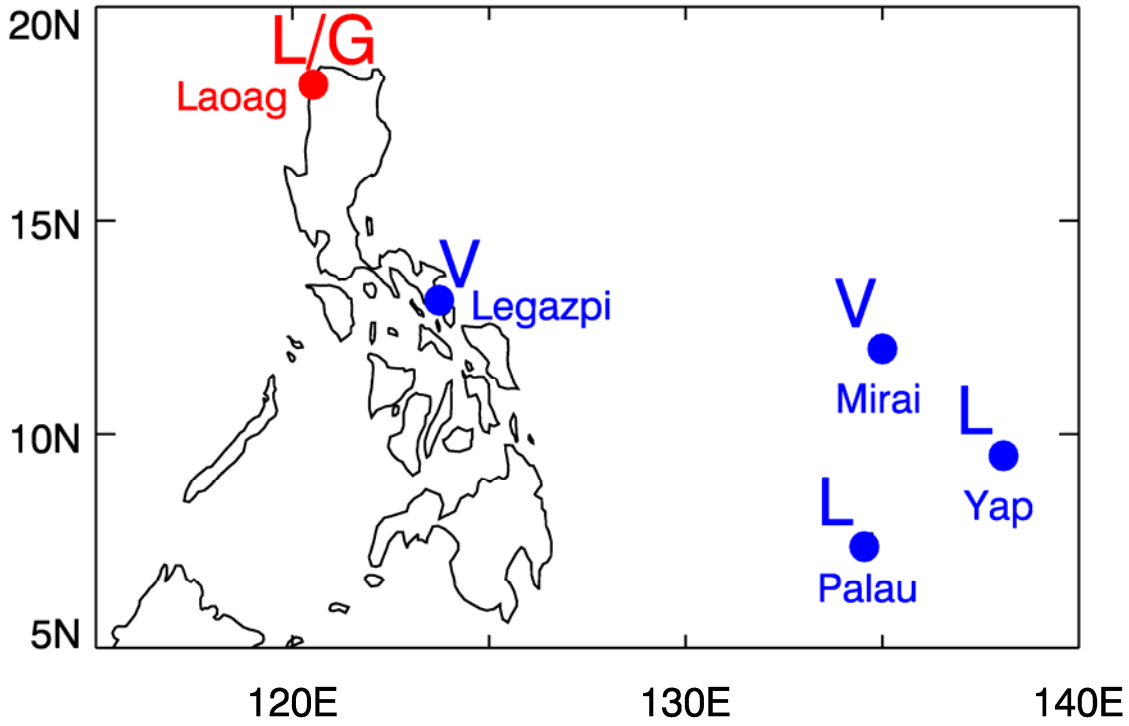

501

502

503 Fig. 1. Map of radiosonde sounding sites during the YMC-BSM 2018 (indicated in red) and

504 2020 (blue) campaigns. Large alphabets indicate radiosonde manufacturer and radiosonde

505 type as of September 2020; L (Lockheed Martin, LMS6), V (Vaisala, RS41), and G (Graw,

506 DFM-09).

507

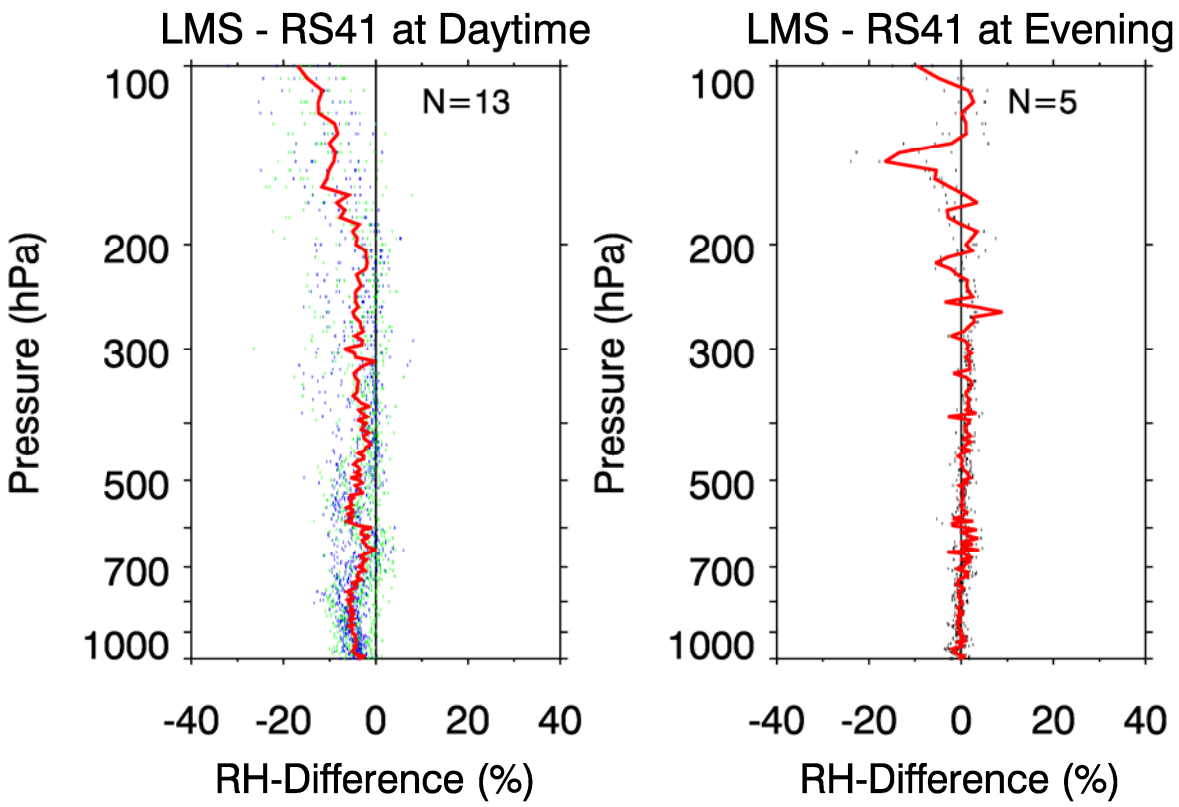

Fig. 2. Relative humidity difference between LMS6 and RS41 (LMS-RS41) for (a) daytime (1100 or 1400 LT), and (b) evening (1700 LT) soundings, respectively. Dots indicate a difference of each sounding (green: 1100 LT, blue: 1400 LT, black: 1700 LT), while red solid line indicates the mean profile.

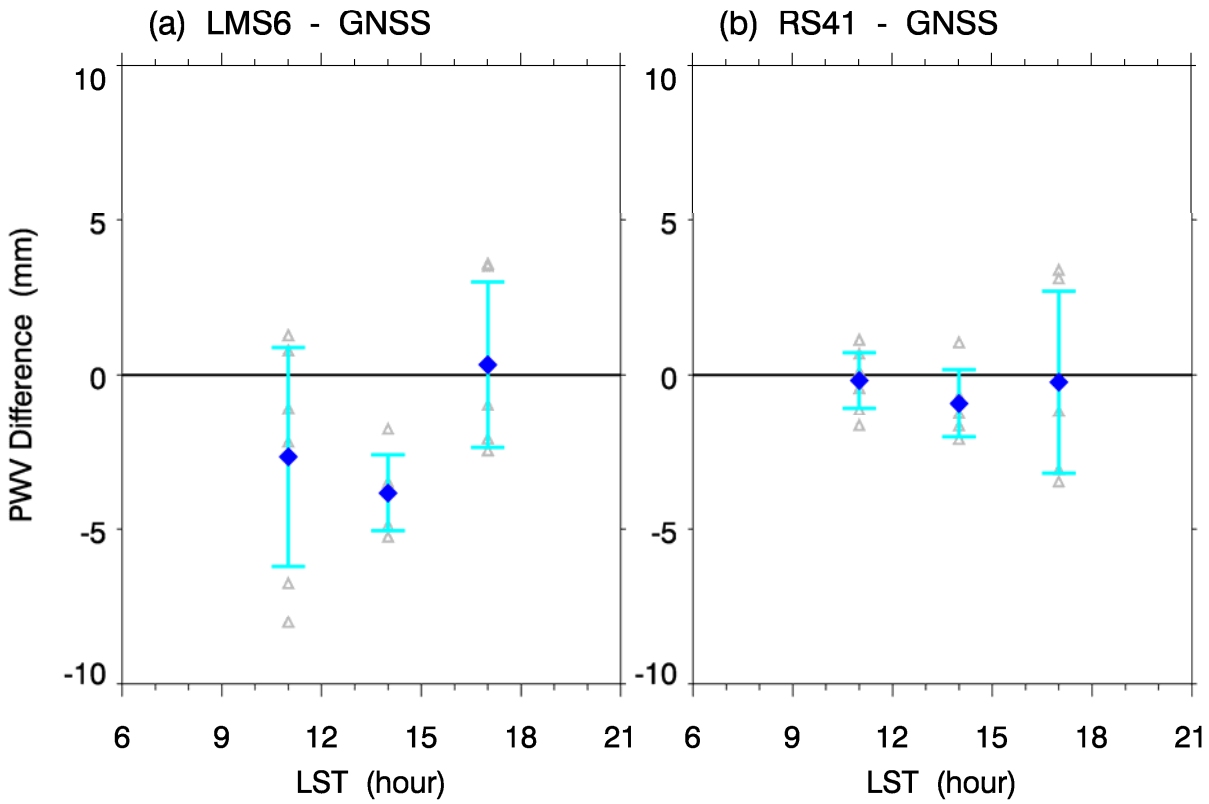

Fig. 3. PWV difference as a function of local time between GNSS-derived PWV and (a) LMS6, and (b) RS41 obtained at Laoag during July 27 - August 3, 2018 as shown in Table 2. Blue diamond, light blue bar, and grey triangle indicate the mean value, standard deviations, and difference at each sounding, respectively. The sample number used are 7 (at 11 LST), 6 (at 14 LST), and 5 (at 17 LST), respectively.

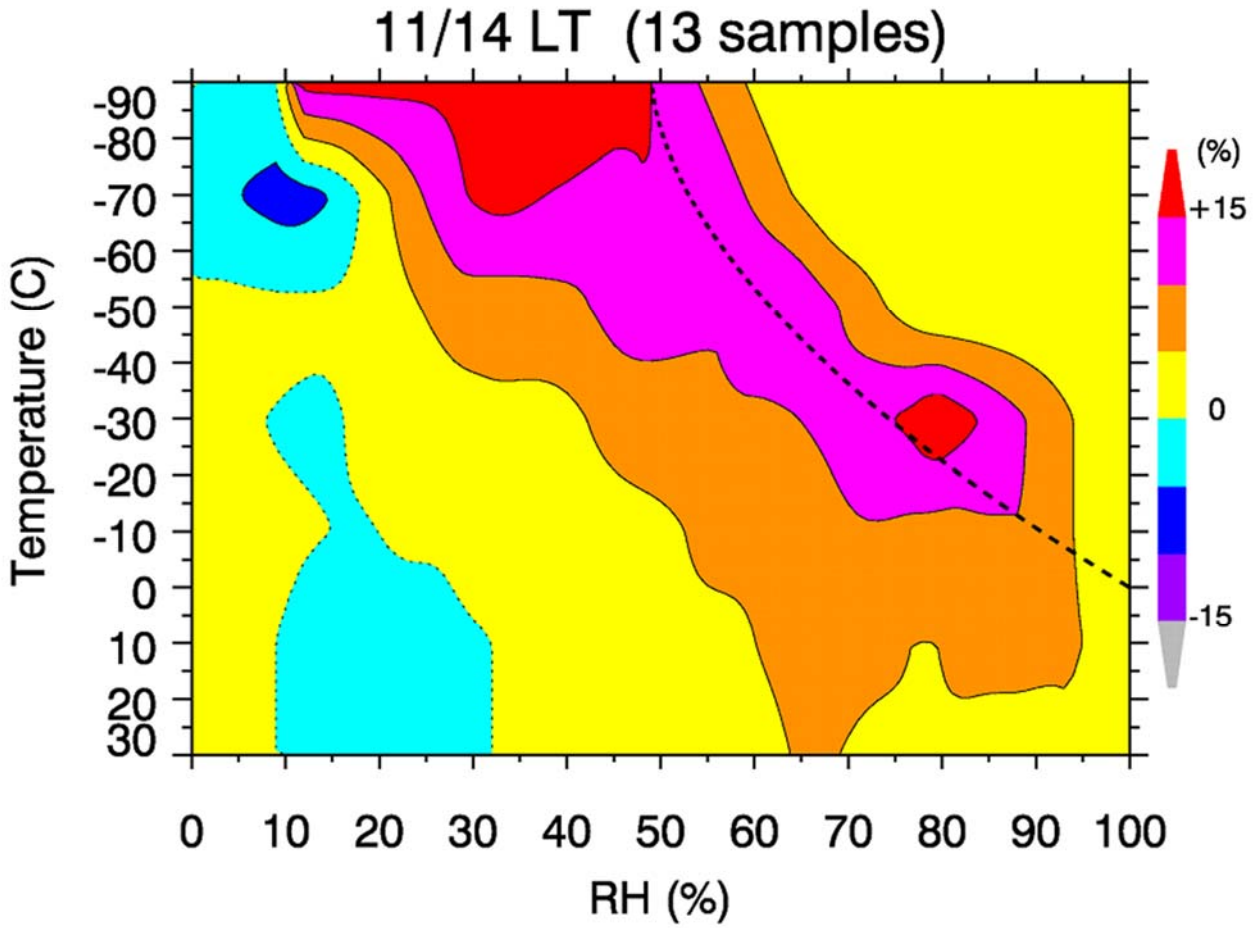

Fig. 4. RH difference between LMS6 and RS41 as a function of RH and temperature based on CDF matching method. Dotted line indicates the saturation with respect to ice.

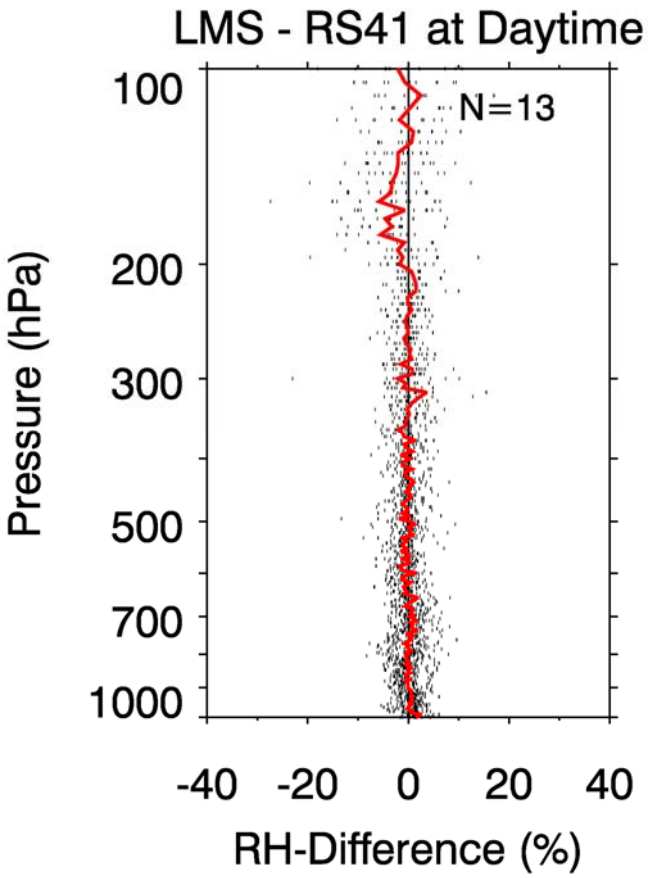

Fig. 5. Same as Fig. 2a, but for corrected values based on CDF matching method.

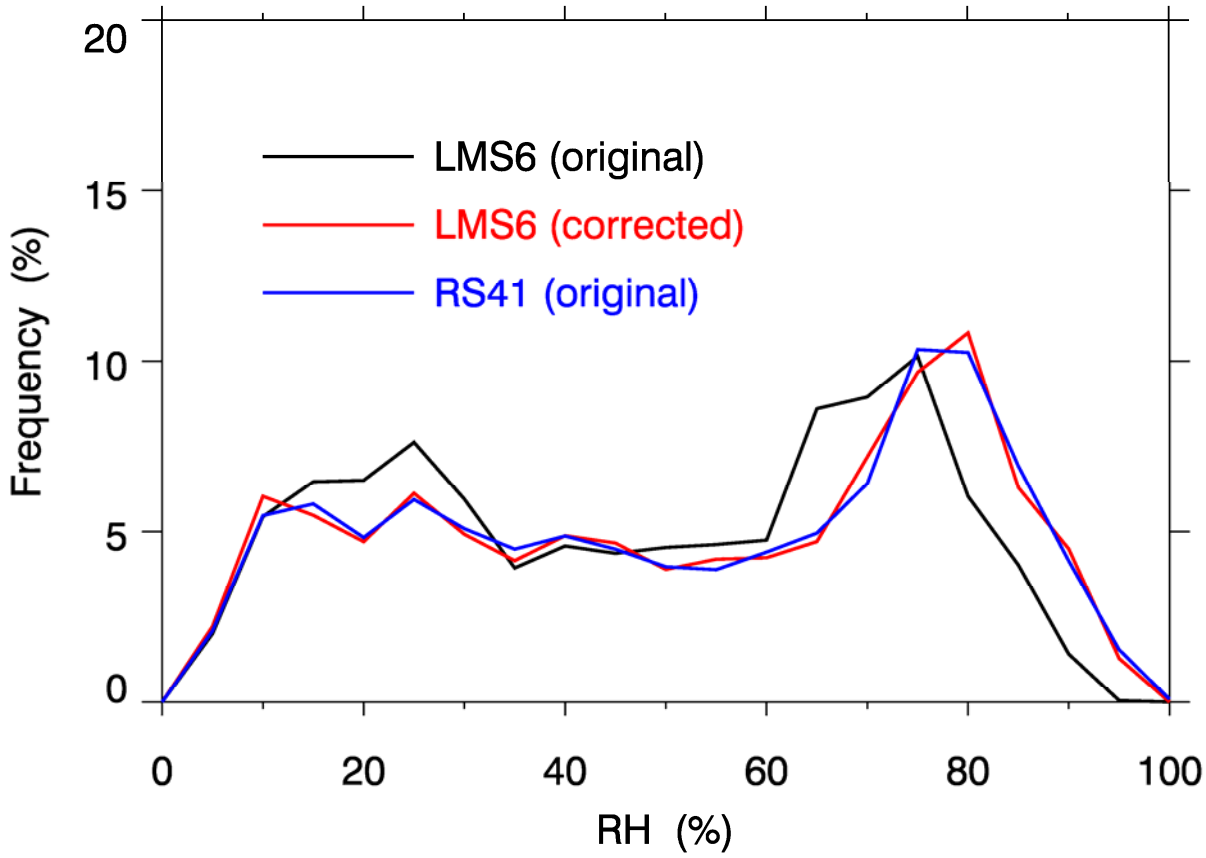

Fig. 6. Frequency distribution of RH binned by 5% for original LMS6 (black), corrected LMS6 (red), and original RS41 (blue). This plot was made using 5hPa interval data between 1000 hPa and 80 hPa from the 13 daytime soundings.

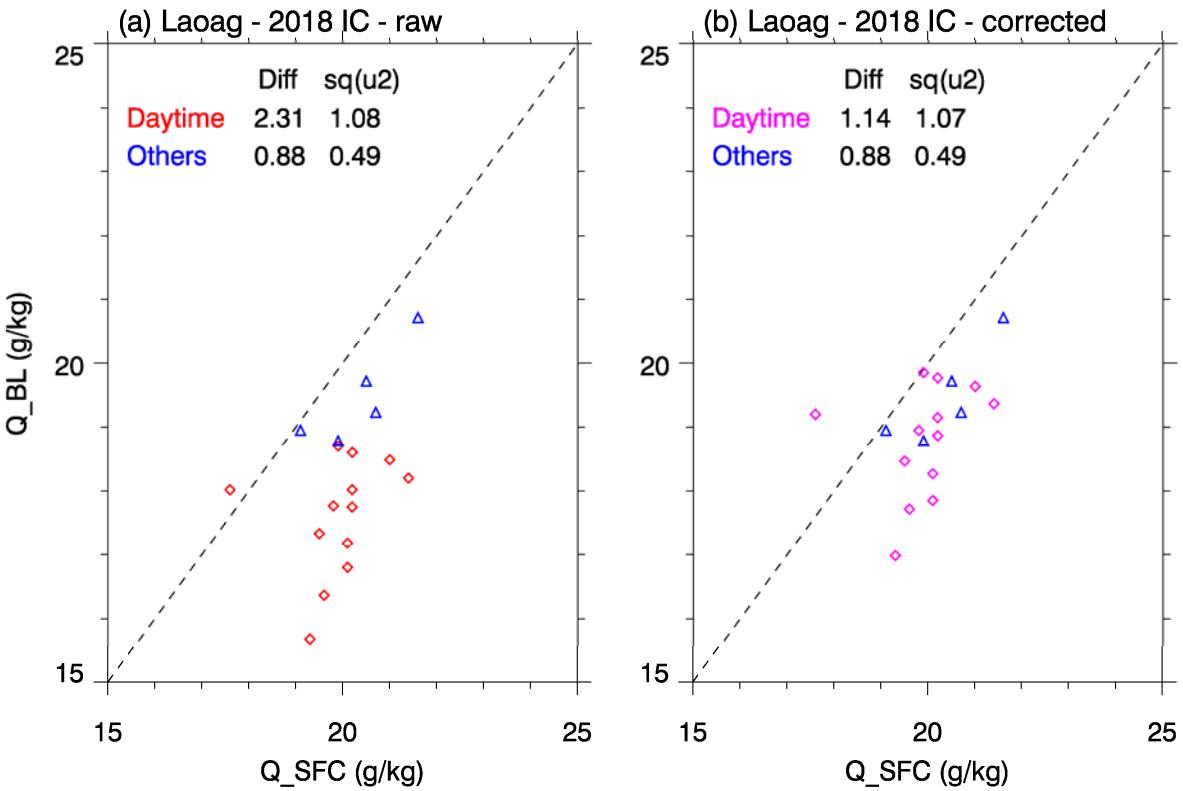

Fig. 7. Scatter plots of specific humidity as a function of surface value measured by surface meteorological station and 300m-mean value above radiosonde initial point for (a) before, and (b) after RH correction. Numbers indicate mean difference (Diff) and square root of unbiased variance from the mean difference (sq(u2)) for 13 daytime soundings and 5 evening soundings in g/kg unit. Since correction is not applied onto non-daytime sounding, “others” in both figures are the same.

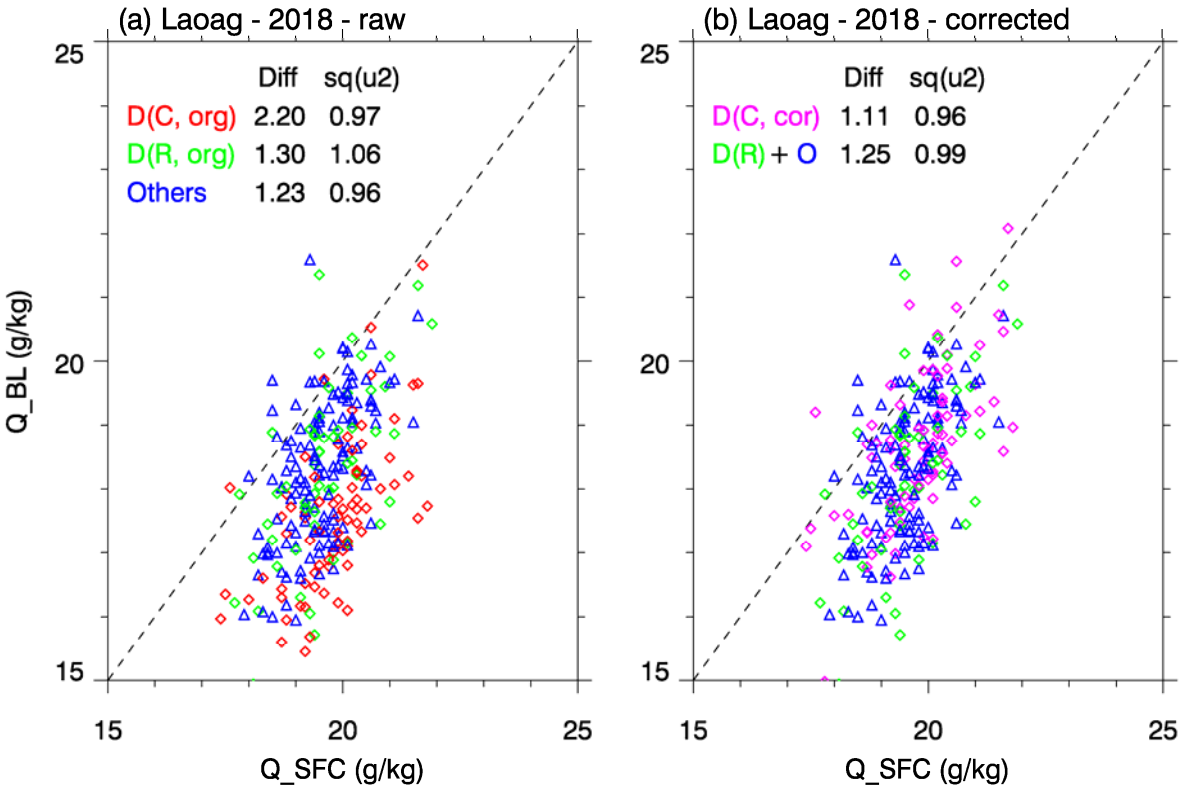

Fig. 8. Same as Fig. 7, but for entire 2 months period during the YMC-BSM 2018. Red/magenta colors indicate the data taken during clear sky daytime for before/after RH correction. Green indicates data taken during cloudy/rainy daytime, while blue indicates evening and nighttime. Clear sky and cloudy/rainy daytime are defined using 93% RH threshold. See more details in the text.

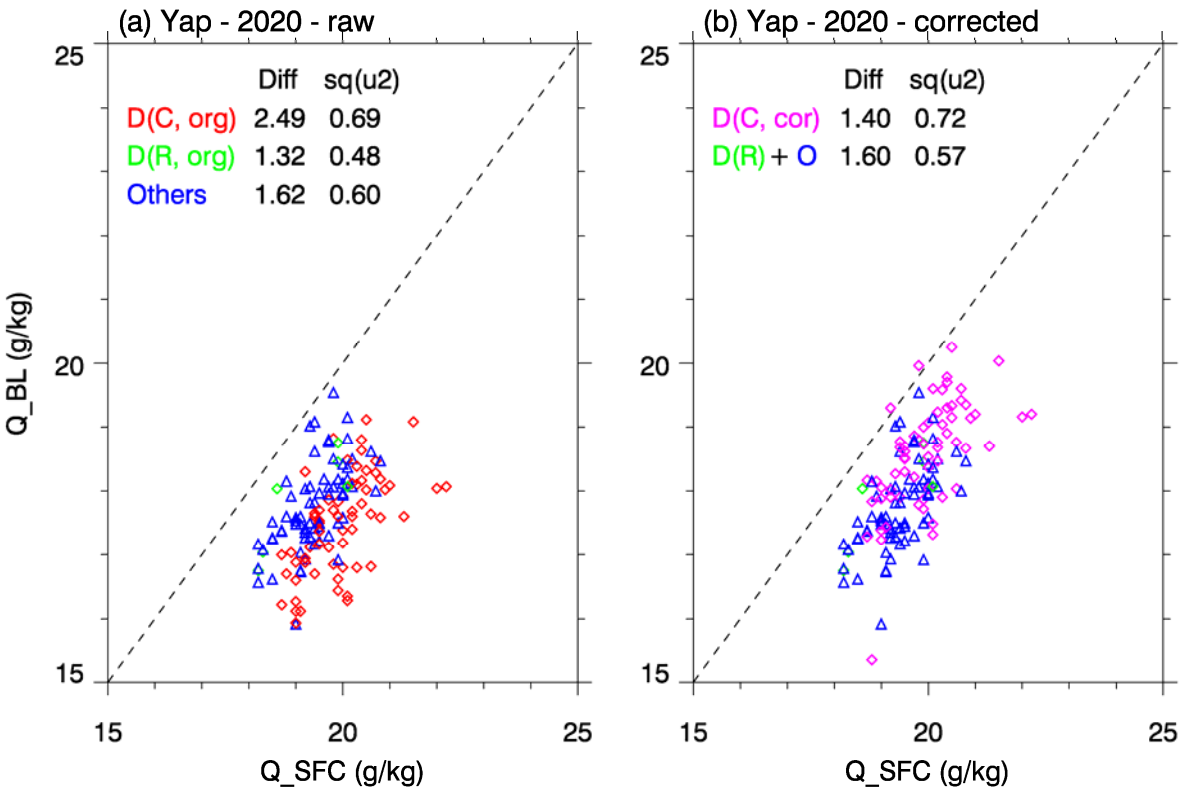

Fig. 9. Same as Fig.8, but for the data obtained at Yap during the YMC-BSM 2020.